Kinin B2 Receptor Mediates Induction of Cyclooxygenase-2 and Is Overexpressed in Head and Neck Squamous Cell Carcinomas

Weiping Zhang,[1] Neil Bhola,[1] Shailaja Kalyankrishna,[1] William Gooding,[3] Jennifer Hunt,[4] Raja Seethala,[4] Jennifer R. Grandis,[1,2,5] and Jill M. Siegfried[1,5]

Departments of [1]Pharmacology and Chemical Biology, [2]Otolaryngology, [3]Biostatistics, and [4]Pathology, [5]University of Pittsburgh School of Medicine and the University of Pittsburgh Cancer Institute, Pittsburgh Pennsylvania

Abstract

Bradykinin has been shown to promote growth and migration of head and neck squamous cell carcinoma (HNSCC) cells via epidermal growth factor receptor (EGFR) transactivation. It has also been reported that bradykinin can cause the induction of cyclooxygenase-2 (COX-2), a protumorigenic enzyme, via the mitogen-activated protein kinase (MAPK) pathway in human airway cells. To determine whether COX-2 is up-regulated by bradykinin in HNSCC, the current study investigated bradykinin-induced EGFR transactivation, MAPK activation, and COX-2 expression in human HNSCC cells. Bradykinin induced a concentration- and time-dependent induction of COX-2 protein in HNSCC, which was preceded by phosphorylation of EGFR and MAPK. These effects were abolished by the B2 receptor (B2R) antagonist HOE140 but not by the B1 receptor (B1R) antagonist Lys-[Leu^8]des-Arg^9-bradykinin. COX-2 induction was accompanied by increased release of prostaglandin E_2. No effect of a B1R agonist (des-Arg^9-bradykinin) on p-MAPK or COX-2 expression was observed. B2R protein was found to be expressed in all four head and neck cell lines tested. Immunohistochemical analysis and immunoblot analysis revealed that B2R, but not B1R, was significantly overexpressed in HNSCC tumors compared with levels in normal mucosa from the same patient. In HNSCC cells, the bradykinin-induced expression of COX-2 was inhibited by the EGFR kinase inhibitor gefitinib or mitogen-activated protein kinase kinase inhibitors (PD98059 or U0126). These results suggest that EGFR and MAPK are required for COX-2 induction by bradykinin. Up-regulation of the B2R in head and neck cancers suggests that this pathway is involved in HNSCC tumorigenesis.

(Mol Cancer Res 2008;6(12):1946–56)

Introduction

G-protein–coupled receptors (GPCR) have been shown to mediate growth of tumor cells in a variety of cancers including small-cell and non–small-cell lung cancer, prostate cancer, and head and neck squamous cell carcinoma (HNSCC). Some of the GPCRs implicated in this process include chemokine receptors, protease-activated receptors, and the receptors for thrombin, bradykinin (bradykinin), and lysophosphatidic acid (1-5). GPCRs are desirable targets for drug development because of the availability of specific targeting agents for these receptors and the overexpression of these receptors in multiple tumor types (6). Hence, there is considerable interest in targeting GPCRs as cancer therapy, alone or in combination with other targeting agents (7, 8).

Bradykinin is one of the GPCRs implicated in HNSCC tumorigenesis, wherein it promotes HNSCC cell migration and proliferation (8). Two types of bradykinin receptors, B1 and B2 bradykinin receptors, have been implicated in tumorigenesis. For example, the B1 receptor (B1R) was up-regulated in malignant prostate (9) and the B2 receptor (B2R) was overexpressed in human gliomas (10) and was detected in gastric, duodenal, lung, and hepatic cancers (11). It has previously been determined which of the bradykinin receptors are present in HNSCC tumors, whether they differ in expression relative to normal mucosal tissue, and which bradykinin receptor contributes to HNSCC tumorigenesis. We therefore investigated the role of B1R and B2R in bradykinin signaling in HNSCC.

GPCRs such as the bradykinin receptor transactivate epidermal growth factor receptor (EGFR), using the potent EGFR signaling pathways to mediate their effects (3). EGFRs have been implicated in linking GPCRs to mitogen-activated protein kinase (MAPK) cascades, which mediate cell proliferative effects (8, 12). Our group has previously shown that in HNSCC cells, bradykinin causes matrix metalloproteinase–mediated release of transforming growth factor α, which transactivates EGFR, and that this pathway is dependent on activation of src (8). Inhibition of EGFR kinase activity prevented bradykinin-induced cell growth and migration of HNSCC, suggesting that EGFR autophosphorylation is

Received 1/10/08; revised 8/14/08; accepted 8/25/08.
Grant support: Head and Neck Cancer Specialized Program of Research Excellence grants P50CA097190 (J.R. Grandis) and R01 CA098372 (J.R. Grandis).
The costs of publication of this article were defrayed in part by the payment of page charges. This article must therefore be hereby marked *advertisement* in accordance with 18 U.S.C. Section 1734 solely to indicate this fact.
Note: Supplementary data for this article are available at Molecular Cancer Research Online (http://mcr.aacrjournals.org/).
Requests for reprints: Jill M. Siegfried, Department of Pharmacology and Chemical Biology, University of Pittsburgh,. E1352, 200 Lothrop Street, Pittsburgh, PA 15261. Phone: 412-623-7769; Fax: 412-648-2229. E-mail: siegfriedjm@upmc.edu.

doi:10.1158/1541-7786.MCR-07-2197

required for this bradykinin function in HNSCC (8). Other studies suggest that EGFR and MAPK are required for the proliferative effects of bradykinin in breast and prostate cancer cells (13, 14). The specific bradykinin receptor required to phosphorylate MAPK through EGFR in HNSCC cells is not known and was explored in this study.

In addition to causing HNSCC proliferation and migration (8), bradykinin has been reported to induce other protumorigenic proteins such as cyclooxygenase-2 (COX-2) in lung cancer cells (15). COX-2 is an important component of HNSCC tumorigenesis; it is overexpressed in HNSCC (16) and its catalyzed product prostaglandin E_2 (PGE_2) is mitogenic for HNSCC (17). Unlike COX-1, which is constitutively present in many tissues, COX-2 is absent or present at very low levels under basal conditions and is induced on stimulation with growth factors or cytokines (18). A cooperative effect of blocking both EGFR and the COX-2 pathway has been observed both *in vivo* and *in vitro* in HNSCC (19). We hypothesized that bradykinin induces COX-2 expression in HNSCC, mediated by activation of MAPK that is dependent on EGFR cross-activation. Our data show that B2R is overexpressed in HNSCC, and that through this receptor, bradykinin transactivates EGFR and uses the MAPK pathway to cause COX-2 induction. B2R overexpression in HNSCC may contribute to release of PGE_2, leading to tumor growth and invasion.

Results

Bradykinin Induces COX-2 Expression in HNSCC Cells

Bradykinin has been reported to induce expression of COX-2 in lung tumor cells (15). We tested whether bradykinin also induces COX-2 in HNSCC cells. Three HNSCC cell lines (PCI-37A, UM-22B, and 1483) were selected to study bradykinin-induced COX-2 expression in a concentration- and time-dependent manner. Treatment of PCI-37A cells with increasing concentration of bradykinin (0.1–1,000 nmol/L) for 2 hours resulted in a concentration-dependent elevation of COX-2 expression. As little as 10 nmol/L bradykinin produced a maximum effect on COX-2 protein levels (2.3-fold increase, $P < 0.05$; Fig. 1A). At higher concentrations, a biphasic

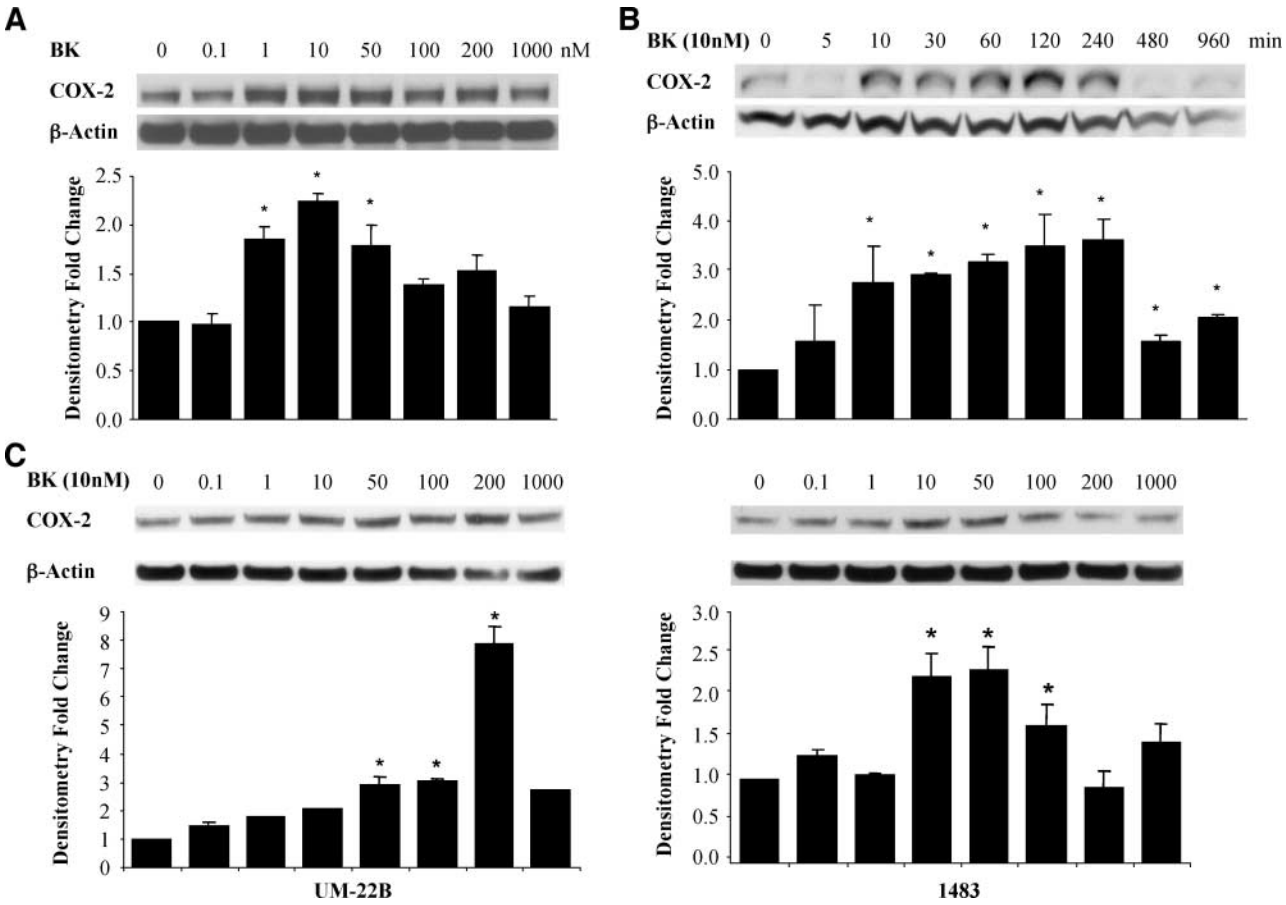

FIGURE 1. Bradykinin-induced COX-2 expression in HNSCC cells. **A.** Dependence of COX-2 expression on bradykinin (*BK*) concentration. PCI-37A cells were serum starved for 48 h and then treated with increasing concentrations of bradykinin (0.1-1,000 nmol/L) for 2 h before harvest. **B.** Time course of bradykinin-induced COX-2 expression. PCI-37A cells were serum starved for 48 h and then treated with10 nmol/L bradykinin for the indicated time intervals. **C.** Bradykinin-induced COX-2 expression in UM-22B and 1483 HNSCC cell lines. UM-22B and 1483 cells were serum starved for 48 h and then treated with increasing concentrations of bradykinin (0.1-100 nmol/L) for 2 h before harvest. Whole-cell lysates were prepared and then immunoblotted with antibodies for COX-2 and β-actin. Representative immunoblots are shown. The graph presents the fold change in protein level compared with control as determined by densitometry (cumulative results from three independent experiments) and correlates to the lane shown directly above each bar. Columns, mean; bars, SE. *, $P < 0.05$, compared with the control.

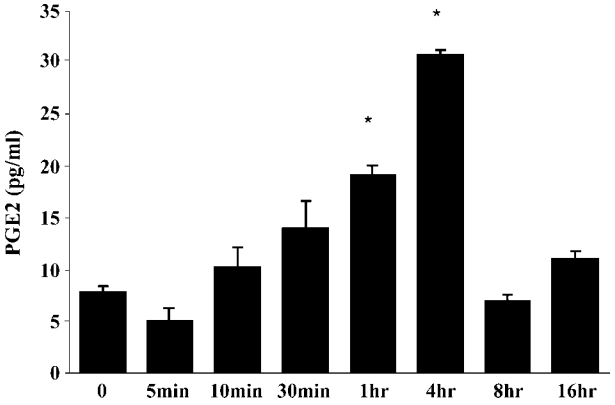

FIGURE 2. Time course of bradykinin-induced PGE_2 release. PCI-37A cells were serum starved for 48 h and then treated with 10 nmol/L bradykinin for the indicated time intervals at 37°C. The cell culture medium was harvested and 50-μL aliquots were used to measure PGE_2 release with an ELISA kit (Cayman Chemicals). Columns, mean from three independent experiments; bars, SE. *, $P < 0.05$, compared with the control.

response was noted, with diminished COX-2 induction at bradykinin treatments >100 nmol/L. Biphasic dose-responses have been noted in bioassays of bradykinin activity (20). Biphasic responses are believed to be mediated by receptor phosphorylation, which shifts the affinity of kinase receptor for ligand and leads to receptor endocytosis (21). Treatment with 10 nmol/L bradykinin for increasing time periods also resulted in a time-dependent induction of COX-2 protein. COX-2 expression was increased by 10 minutes after bradykinin addition and reached maximal levels by 2 to 4 hours (3.8-fold induction, $P < 0.05$; Fig. 1B). Bradykinin induced a similar concentration-related increase in COX-2 expression in HNSCC cell lines UM-22B (3-fold increase, $P < 0.05$; Fig. 1C, *left*) and 1483 (2.4-fold increase, $P < 0.05$; Fig. 1C, *right*). Three independent experiments were carried out for each condition. UM-22B cells, which contain lower B2R expression levels (see Fig. 6), were less sensitive to bradykinin stimulation.

COX-2 induction has been frequently found to be caused by increased mRNA synthesis (22). We showed by reverse transcription-PCR analysis that COX-2 mRNA expression increased up to 2-fold between a 30 minute and 2 hour time period after bradykinin treatment between 1 nmol/L and 1 μmol/L. A biphasic response was also noted in mRNA induction, with diminished mRNA found at 1 μmol/L compared with lower concentrations (see Supplementary Fig. S1A and B).

PGE_2 Release Is Enhanced in Response to Bradykinin-Induced COX-2 Expression

COX-2 catalyzes the rate-limiting step of arachidonic acid conversion to prostaglandins, including PGE_2. PGE_2 is the major biologically active product of the COX-2 pathway (20) and increases cell proliferation and motility. We determined whether PGE_2 is released in conjunction with bradykinin-stimulated COX-2 expression. PCI-37A cells were cultured in the presence of bradykinin (10 nmol/L), and culture supernatants were collected at various time points up to 16 hours. As shown in Fig. 2, there was a time-dependent accumulation of PGE_2 that became significant after 1 hour ($P < 0.05$), peaked at 4-fold higher than baseline at 4 hours, and declined after 4 hours of treatment. These results were observed in two replicate experiments and show that bradykinin activation of COX-2 in HNSCC is accompanied by PGE_2 release.

At 8 and 16 hours, there is still an elevation of COX-2 protein as seen in Fig. 1B, but PGE_2 levels released into the culture medium were at basal values. This could be due to low sensitivity of the ELISA assay, internalization of PGE_2 by binding to its receptors (because HNSCC cells respond to PGE_2; ref. 8), or lack of PGE_2 precursor at the later time points. In two experiments using 1 μmol/L bradykinin, only slight increases in PGE_2 release (10-12 pg/mL) were observed over a 16-hour time period, in agreement with the biphasic responses we observed in COX-2 expression (data not shown).

Bradykinin Induces MAPK Phosphorylation

Bradykinin has previously been shown to mediate EGFR transactivation (3, 8), which can result in phosphorylation of

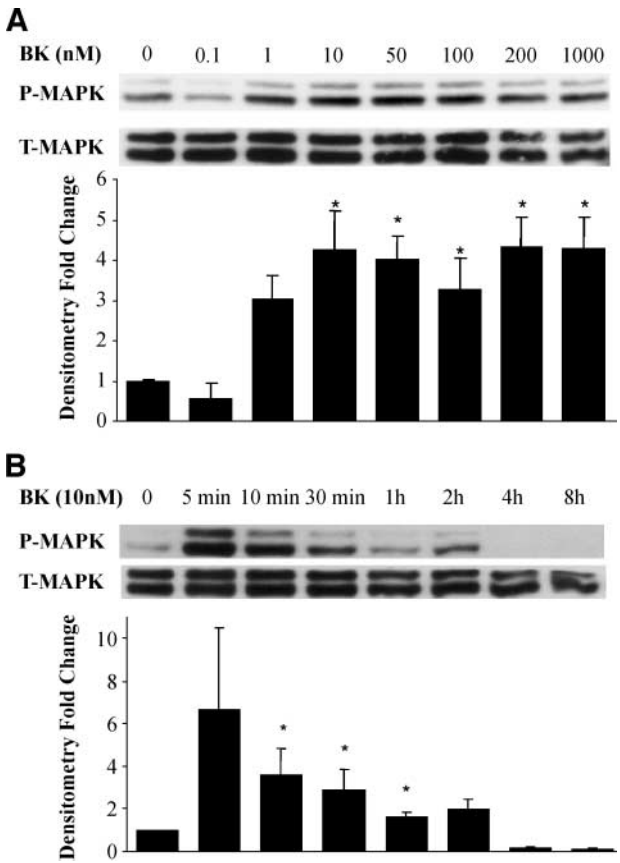

FIGURE 3. Bradykinin-induced phosphorylation of MAPK. **A.** Dependence of MAPK activation on bradykinin concentration. PCI-37A cells were serum starved for 48 h and then treated with increasing concentrations of bradykinin (0.1-1,000 nmol/L) for 10 min before harvest. **B.** Time course of bradykinin-induced p-MAPK. PCI-37A cells were serum starved for 48 h and then treated with 10 nmol/L bradykinin for the indicated time intervals (0-8 h). Whole-cell lysates were prepared and then immunoblotted with antibodies for p-MAPK and total MAPK. Representative immunoblots are shown. The graph presents the fold change in protein level compared with control as determined by densitometry (cumulative results from three independent experiments) and correlates to the lane shown directly above each bar. Columns, mean; bars, SE. *, $P < 0.05$, compared with the control.

MAPK. Under similar conditions that result in COX-2 induction in HNSCC cells, bradykinin also caused activation of MAPK in a time- and concentration-dependent manner. We found that phospho-MAPK was increased significantly above baseline and was maximal at a concentration of 10 nmol/L bradykinin (Fig. 3A); the increase occurred within 5 to 10 minutes of bradykinin addition in PCI-37A cells ($P < 0.05$; Fig. 3B) and declined over 1 to 2 hours. Thus, maximal activation of MAPK occurred at the same concentration of bradykinin as the induction of COX-2, and appearance of phospho-MAPK preceded COX-2 induction. Results are from three independent experiments. We did not observe a biphasic response in phospho-MAPK induction, which may not occur because phosphorylation of MAPK occurs rapidly, before desensitization induced by higher concentrations of bradykinin is complete. MAPK activation is necessary for COX-2 induction (see Fig. 5C) but may not be sufficient because it is not diminished at concentrations of bradykinin that show weak ability to induce COX-2 mRNA and protein. In our previous study of COX-2 induction by hepatocyte growth factor (22), we found both MAPK and p38 were required and participated in phosphorylating multiple transcription factors that bind the COX-2 promoter, most likely at more than one phosphorylation site. Inhibition of either MAPK or p38 prevented COX-2 induction (22). It is possible that biphasic responses to bradykinin are present in other steps that are also needed for COX-2 induction in HNSCC cells.

Bradykinin Mediates Signaling through B2R

Bradykinin is an agonist for B2R and signals primarily through this receptor. Although bradykinin does not have affinity for B1R, it can be metabolized by kinin to des-Arg^9-bradykinin, which activates B1R (23). Moreover, the B1R and B2R can exhibit cross talk with each other at the level of heterotrimeric G-proteins (13). To determine the receptor subtype involved in bradykinin signaling in HNSCC, the cells were pretreated with increasing concentrations of the B2R antagonist HOE140, which is highly selective for the B2R with a K_i <0.5 nmol/L and virtually no affinity for the B1R (24) or the highly selective B1R antagonist Lys (Des-Arg^9-Leu^8) bradykinin, which has a K_i for B1R in the nanomolar range and a >10,000-fold lower affinity for the B2R (25), followed by treatment with bradykinin. The B2R antagonist, but not the B1R antagonist, inhibited bradykinin-induced EGFR and MAPK activation and COX-2 induction (Fig. 4). Figure 4A depicts EGFR tyrosine phosphorylation in HNSCC after treatment with bradykinin, assessed after immunoprecipitation with an anti-EGFR antibody. Tyrosine phosphorylation of EGFR was enhanced 10-fold by treatment with 10 nmol/L bradykinin. Bradykinin-activated EGFR tyrosine phosphorylation was inhibited 70% by 10 μmol/L HOE140. However, phosphorylation of EGFR was not appreciably inhibited by pretreatment with concentrations of B1R antagonist up to 10 μmol/L. Likewise, the B2R antagonist, but not B1R antagonist, inhibited MAPK activation (Fig. 4B). An 80% reduction in p-MAPK was observed with HOE140 ($P < 0.01$), whereas the B1R antagonist had no effect ($P > 0.05$, not significant). The effect of bradykinin-induced COX-2 protein expression was also significantly reduced by HOE140 but not by B1R antagonist. Bradykinin-induced COX-2 levels measured are below baseline ($P = 0.002$) when cells are pretreated with HOE140 at ≥0.1 μmol/L, but B1R antagonist shows no effect ($P = 0.48$ with B1R antagonist from 1 to 50 μmol/L, Fig. 4C). These results support the role of the B2R, and not the B1R, in mediating COX-2 induction after treatment with bradykinin.

To confirm that COX-2 protein expression and MAPK activation were not regulated by B1R, we examined p-MAPK and COX-2 protein levels following treatment of PCI-37A cells with increasing concentrations of B1R agonist (des-Arg^9-bradykinin). As shown in Fig. 4D, the B1R agonist had no effect on either p-MAPK activation or COX-2 expression in PCI-37A cells after B1R agonist (des-Arg^9-bradykinin) treatment.

EGFR and MAPK Are Required for COX-2 Induction by Bradykinin

Because bradykinin activates the EGFR pathway, we next tested the contribution of this pathway to COX-2 induction. We pretreated PCI-37A cells with EGFR tyrosine kinase inhibitor gefitinib for 30 minutes before addition of 10 nmol/L bradykinin. We found that the bradykinin-induced COX-2 was significantly abrogated in the presence of 1 μmol/L gefitinib (71.4% inhibition, $P < 0.05$; Fig. 5A). EGFR also seemed to contribute to the baseline expression of COX-2 because either agent alone decreased the basal COX-2 protein levels.

Bradykinin is known to activate EGFR by a src-dependent release of EGFR ligand in HNSCC (8). We confirmed that under the conditions used for EGFR activation and COX-2 induction in HNSCC cells, the effect of bradykinin on EGFR phosphorylation was inhibited by blocking the external EGFR ligand binding site with the antibody C225 (Fig. 5B, *left*). Bradykinin-induced activation of PY1068-EGFR was blocked >90% by C225. Published data from our laboratory have shown that the EGFR ligand most likely responsible for mediating bradykinin effects is transforming growth factor-α (8). The EGFR inhibitor gefitinib also completely blocked formation of PY1068-EGFR (Fig. 5B, *right*), suggesting the effect is due to autophosphorylation of EGFR, rather than to a different kinase. This is consistent with a response mediated by EGFR ligand. Because bradykinin activates the src-EGFR pathway, we also tested the contribution of this pathway to COX-2 induction (Fig. 5A). We found that bradykinin-induced increase in COX-2 was also abrogated by pretreatment with the src inhibitor AZD0530 (81% inhibition, $P < 0.05$). These results suggest that both src and EGFR are involved in COX-2 induction by bradykinin. Inhibition of src alone or inhibition of EGFR alone was sufficient to abrogate COX-2 induction, suggesting that these two molecules act in the same pathway, rather than through independent pathways, to induce COX-2. We previously reported that src is activated by GPCR ligands and is responsible for the activation of proteases that cleave EGFR proligands to their active forms in HNSCC, providing a mechanism for EGFR activation (17).

Because MAPK is downstream of EGFR activation, we explored whether MAPK activation is required for bradykinin-induced COX-2 expression. Two mitogen-activated protein

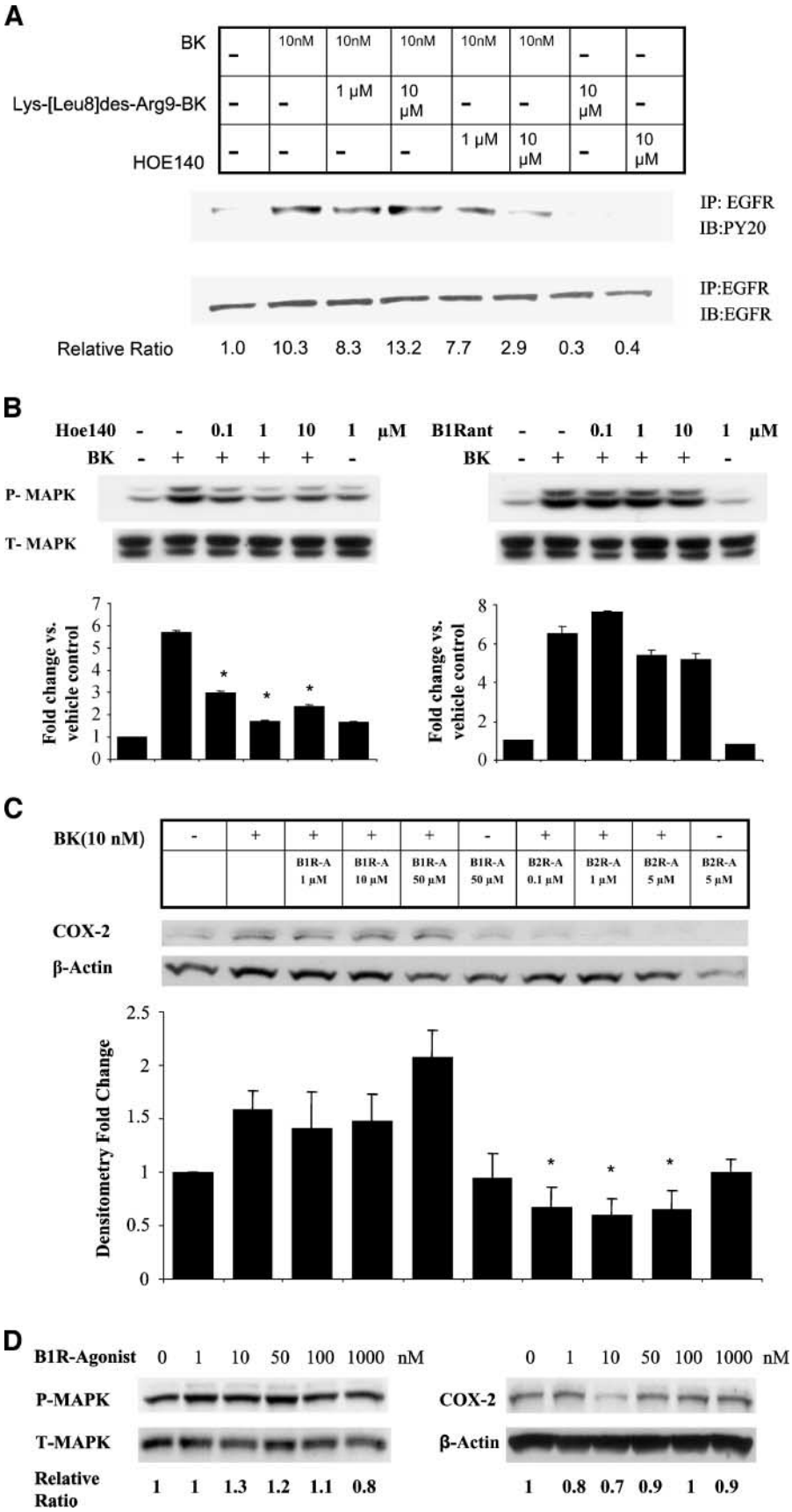

FIGURE 4. Bradykinin-induced phosphorylation of EGFR and MAPK and COX-2 expression is mediated through B2 bradykinin receptor but not B1 bradykinin receptor. **A.** Bradykinin-induced phosphorylation of EGFR in the presence of bradykinin receptor antagonists. **B.** Bradykinin-induced phosphorylation of MAPK in the presence of bradykinin receptor antagonists. **C.** Bradykinin-induced COX-2 expression in the presence of bradykinin receptor antagonists. PCI-37A cells were serum deprived for 3 d, pretreated with a range of concentrations of B1 receptor antagonist Lys-(Des-Arg^9-Leu^8)-bradykinin or B2-receptor antagonist HOE140 as indicated for 1 h, followed by treatment with 50 nmol/L bradykinin for 5 min for detection of phospho-EGFR and phospho-MAPK and with 10 nmol/L bradykinin for 2 h for measurement of COX-2. Whole-cell lysates were prepared, and phospho-EGFR, phospho-MAPK, and COX-2 levels were determined by immunoblotting with specific antibodies as described in Materials and Methods. Relative ratios of p-MAPK or COX-2 expression versus total MAPK or β-actin expression were calculated. Representative immunoblots are shown. The graph presents the fold change in protein level compared with control as determined by densitometry (cumulative results from three independent experiments) and correlates to the lane shown directly above each bar. Columns, mean from two independent experiments; bars, SE. *, $P < 0.05$, compared with bradykinin treatment. **D.** Effect of B1R agonist on p-MAPK and COX-2 expression. PCI-37A cells were serum deprived for 2 d, treated with a range of concentrations of B1R agonist des-Arg^9-bradykinin for 10 min for p-MAPK (*left*) and for 2 h for COX-2 (*right*). Methods used were identical to those described above for **A** to **C**. This is a representative experiment that was repeated two additional times with similar results.

kinase kinase (MEK) inhibitors, PD98059 and U0126, were used, both of which block phosphorylation of MAPK by MEK. We measured the effect of PD98059 and U0126 on bradykinin-induced expression of COX-2 (Fig. 5C). Pretreatment of PCI-37A cells with PD98059 (1-50 μmol/L) or U0126 (1-50 μmol/L) for 30 minutes before addition of 10 nmol/L bradykinin caused a significant reduction of bradykinin-induced COX-2 expression in a concentration-dependent manner. When cells were pretreated with 1 μmol/L PD98059, bradykinin-induced COX-2 expression was inhibited by 85%, whereas in cells pretreated with 1 or 10 μmol/L U0126, bradykinin-induced COX-2 expression was also reduced 85% ($P < 0.05$; Fig. 5C). These results confirm that MAPK activation is upstream of bradykinin-induced COX-2 expression.

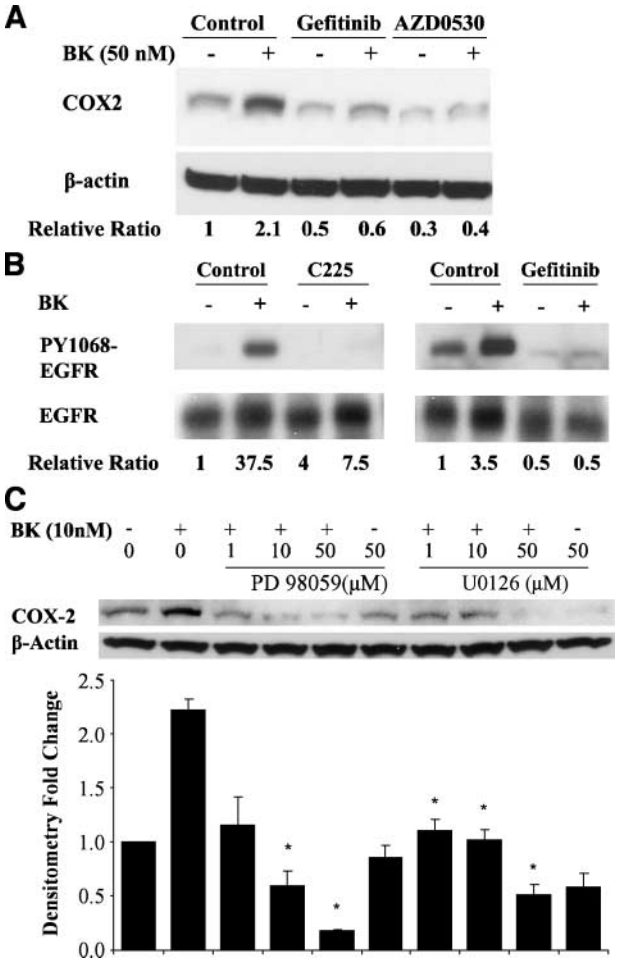

FIGURE 5. EGFR and MAPK are required for COX-2 induction by bradykinin. PCI-37A cells were serum deprived for 3 d followed by subsequent treatments. **A.** Bradykinin-induced COX-2 expression in the presence of an EGFR or a src inhibitor. Cells were pretreated for 60 min with vehicle, the src inhibitor AZD0530 (1 μmol/L), or the EGFR tyrosine kinase inhibitor gefitinib (1 μmol/L) followed by treatment with bradykinin (50 nmol/L) for 2 h, and COX-2 protein levels were analyzed by immunoblotting. Relative ratios of COX-2 expression versus β-actin expression were calculated from two independent experiments. **B.** Effect of EGFR inhibition on phosphorylation of EGFR in response to bradykinin. Cells were preincubated with vehicle, the EGFR antibody C225 (100 nmol/L), or the EGFR tyrosine kinase inhibitor gefitinib (1 μmol/L) for 5 min and then treated with bradykinin (50 nmol/L) for 10 min. EGFR phosphorylation at a representative autophosphorylation site, Y1068, and total EGFR were analyzed by immunoblotting. Relative ratios of p-EGFR (PY1068) phosphorylation versus total EGFR were calculated. This is a representative experiment that was repeated two additional times with similar results. **C.** Bradykinin-induced COX-2 expression in the presence of MEK inhibitors. Cells were pretreated with vehicle or MEK inhibitors PD 098059 (1-50 μmol/L) or U0126 (1-50 μmol/L) for 1 h before treatment with 10 nmol/L bradykinin for another 2 h, and COX-2 expression was determined by immunoblotting with COX-2 antibody. Representative immunoblots are shown. The graph presents the fold change in protein level compared with control as determined by densitometry (cumulative results from three independent experiments) and correlates to the lane shown directly above each bar. Columns, mean; bars, SE. *, $P < 0.05$, compared with the bradykinin treatment.

B2R Is Overexpressed in HNSCC Tumors

Because B2R was found to mediate signaling by bradykinin in HNSCC cells, we examined the expression of B2R in HNSCC cell lines and found that B2R was expressed in all three HNSCC tumor cell lines tested, 1483, UM-22B, and PCI-37A, as well as in an immortalized cell line derived from normal mucosa of the esophagus, HET1A (Fig. 6A). This is in accordance with previous reports that B2R is ubiquitously present even in normal tissue (26). The level of B2R protein was found to be 2.2, 1.6, and 2.6 times higher when normalized for β-actin in the 1483, UM-22B, and PCI-37A tumorigenic cells, respectively, compared with the HET1A cells. This suggests that B2R is overexpressed in HNSCC tumors.

To determine whether B2R levels are modulated in HNSCC tumors, we compared the proteins levels of B2R in lysates of six HNSCC primary tumors and corresponding normal mucosa from the same patients. Immunoblot analysis revealed that B2R expression was higher on average in tumors by 2.8-fold as compared with normal mucosa (Fig. 6B). B2R levels in paired tumor tissue and normal mucosal tissue from 43 patients were also compared by immunohistochemical staining. The clinical and pathologic characteristics of 43 patients whose HNSCC samples were analyzed for B2R staining are shown in Table 1. B2R staining was found primarily in the tumor cells and was undetectable in the stroma (Fig. 6C). Low levels of B2R staining were observed in normal tissue. Wilcoxon signed rank analysis of immunohistochemistry mean staining intensity values revealed that B2R levels were 3-fold higher in tumor tissue compared with normal control tissue and the difference was statistically significant (Fig. 6C; $P = 0.045$). B1R was detected by immunohistochemistry in only a small percentage of tumor and normal tissues and did not show statistical differences, suggesting that the B1R is not significantly expressed in HNSCC (data not shown). These results show that B2R, but not B1R, is overexpressed in head and neck tumor, compared with control normal tissue from the same patient, and confirms results seen in cell lines.

B2R Levels in HNSCC Do Not Correlate with Clinical Characteristics

Many tumorigenic signaling molecules such as EGFR are up-regulated on disease progression, and an increase in their levels correlates with poor prognosis and decreased survival (27). We investigated the possibility that B2R levels (measured as staining intensity by immunohistochemistry) in HNSCC may correlate with patient survival or with tumor stage. However, there was no significant correlation between median survival or

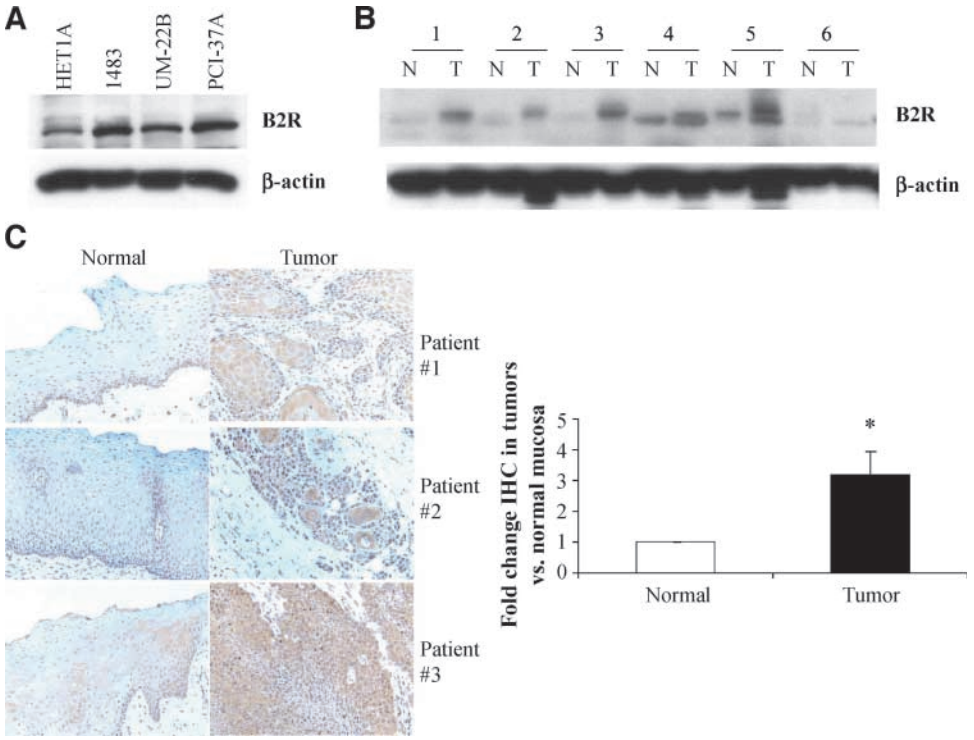

FIGURE 6. B2R is overpressed in head and neck cancer. **A.** HNSCC cell lines. Cell lysates from an immortalized normal mucosa cell line, HET1A, and three HNSCC cell lines, 1483, UM-22B, and PCI-37A, were subjected to immunoblot analysis to determine B2R levels and then reprobed with β-actin. **B.** HNSCC tumors compared with normal mucosa by immunoblot. Lysates of HNSCC tumors and corresponding control normal mucosa obtained from six patients were probed for B2R levels by immunoblotting and reprobed with β-actin antibody. **C.** Immunohistochemistry of B2R expression in tumor tissue compared with normal mucosa from same patient. Immunohistochemical staining of B2R was done in tumor tissue and control normal mucosa from 43 HNSCC patients (tissue sections from three representative patients). The staining intensity was scored as described in Materials and Methods, and *P* value was computed using the Wilcoxon matched pairs sign rank test.

time to progression and B2R intensity (log-rank $P = 0.88$) or B2R weighted intensity (log-rank $P = 0.48$). There was also no correlation between B2R intensity and T stage ($P = 0.14$) or N stage ($P = 0.8$) of the tumor or smoking status ($P = 0.66$) of the patient. These data suggest that B2R up-regulation is not restricted to tumors from patients with tobacco exposure or with HNSCC disease progression. How early in the course of HNSCC tumor development B2R overexpression occurs remains to be determined.

Similarly, there was also no correlation between patient survival and B1R intensity (log-rank $P = 0.1$) or B1R weighted intensity (log-rank $P = 0.24$). Thus, not only is B1R poorly expressed in HNSCC but also its expression level does not correlate with disease prognosis.

Discussion

Our findings that B2R is overexpressed in HNSCC and has important biological functions, including induction of the protumorigenic enzyme COX-2, support the involvement of this GPCR in HNSCC tumorigenesis. Kinins such as bradykinin and kallidin, as well as the bradykinin receptors, have previously been implicated in inflammation and hyperalgesia, and recently a role for these receptors in tumorigenesis has been identified (26). B2R knockout mice showed decreased growth of tumor xenografts due to reduced angiogenesis (28). It is thought that B2Rs are expressed constitutively by a variety of cells whereas B1Rs are induced in response to inflammation and injury. In contrast, our study revealed insignificant levels of B1R in HNSCC tumors, whereas B2R was overexpressed in HNSCC. Similar to our findings, B2R levels have been found to be overexpressed in human gliomas, where they increase with increasing tumor grade (10). However, in our study, there was no correlation between the level of B2R expression and HNSCC tumor stage or survival, suggesting that multiple pathways besides B2 signaling contribute to HNSCC tumorigenesis. In our study, B2R was expressed exclusively in HNSCC tumor cells and was not detected in the stroma. This is in contrast to esophageal carcinoma where giant cells and mast cells infiltrating the tumor expressed B2R (29). In addition, we did not observe any microvessel staining of B2R, although B2Rs have been implicated in angiogenesis (28) and increase in vascular permeability. Supporting our finding of B2R expression in tumor cells of HNSCC patients, we found that B2R was expressed and mediated tumorigenic signaling in cultured HNSCC cell lines. Thus, the role of B2R in tumorigenesis seems to vary depending on the tumor type; in HNSCC, its role seems to be restricted to tumor cells.

COX-2 is thought to be responsible in different types of inflammation and tumorigenesis. COX-2 is an important target for chemoprevention in HNSCC and other tumors (30). Induction of COX-2 often serves as an amplification

mechanism for proliferative signaling. For example, the product of COX-2, PGE2, itself increases COX-2 levels through its GPCR, generating a positive feedback loop (31). It seems that bradykinin also uses COX-2 to amplify its tumorigenic effect in HNSCC. In this study, we found that treatment of head and neck cancer cells with bradykinin induced subsequent activation of EGFR, MAPK, and expression of COX-2. These findings are consistent with our previous study in HNSCC (8), in which we showed that bradykinin induced EGFR ligand release and activated EGFR downstream signaling. In this previous report, we also found that MAPK induction by bradykinin was inhibited by a small-molecule EGFR tyrosine kinase inhibitor and C225, showing the involvement of EGFR in bradykinin-induced MAPK signaling in HNSCC. We also detected some EGFR-independent signaling by bradykinin to MAPK (8), suggesting that there may be additional mechanisms of MAPK activation by bradykinin. However, in the studies reported here, B2R antagonist, EGFR inhibition, and MEK inhibitors all prevented bradykinin-induced COX-2 expression, suggesting that the bradykinin-EGFR-MAPK signaling axis is upstream of COX-2. It is possible that other molecules besides EGFR participate in bradykinin induction of MAPK, but probably not in signaling complexes that activate COX-2. These results suggest that the EGFR/MAPK signaling pathway is required for the induction of COX-2 caused by bradykinin. In addition, there is no effect on activation of MAPK and expression of COX-2 when HNSCC cells were treated with B1R agonist. This further supports the involvement of B2R, but not B1R, in bradykinin signaling in HNSCC.

We also found that the autophosphorylation of EGFR site Y1068 in response to bradykinin is most likely mediated through extracellular ligand release because it was inhibited by the EGFR antibody C225, which blocks the external ligand binding site. Previous studies from our group have shown that bradykinin-mediated regulation of total EGFR phosphorylation is mediated through Src family kinase–dependent activation of a metalloproteinase, tumor necrosis factor-α converting enzyme, which releases transforming growth factor-α to activate EGFR (8). Therefore, it is very likely that bradykinin-mediated EGFR autophosphorylation also involves tumor necrosis factor-α converting enzyme activation and transforming growth factor-α release. Phosphorylation of EGFR at different sites leads to differential recruitment of signaling molecules. For example, phosphorylation of EGFR at Y1068 leads to recruitment of a shc/Grb/SOS complex (32), whereas phosphorylation at Y845 results in STAT5b activation (33). Previous studies from our group have shown that inhibition of EGFR kinase activity using erlotinib or gefitinib inhibited bradykinin-induced MAPK activation, cell growth, and migration of HNSCC (8), suggesting that EGFR autophosphorylation is required for bradykinin function in HNSCC. It is very likely that abrogation of EGFR phosphorylation will also inhibit the effects of bradykinin on growth, similar to reports on other GPCRs in cancer cells (34).

Table 1. Demographics of HNSCC Patients Analyzed for B2R Staining

	n (%)
Smoking status	
Smokers	29 (67.4)
Nonsmokers	3 (7)
Unknown smoking status	11 (25.6)
Age (y)	
31-40	2 (4.7)
41-50	5 (11.6)
51-60	9 (20.9)
61-70	19 (44.2)
71-80	7 (16.3)
81-90	1 (2.3)
Cancer type	
Primary	36 (83.7)
New primary	2 (4.7)
Recurrence	5 (11.6)
Race	
Caucasian	40 (93)
African American	3 (7)

The signaling routes linking GPCRs to MAPK often involve EGFR tyrosine kinase phosphorylation. We show that a similar cross talk involving activation of the EGFR/MAPK pathway by bradykinin results in increased levels of COX-2. Overexpression of COX-2 often acts as an amplification mechanism for proliferation. For example, p60-v-src transformation of 3T3 fibroblasts results in high COX-2 levels (35). EGFR mediates expression of COX-2 in response to tobacco smoke exposure in oral cells (36). COX-2 is an important target for chemoprevention in HNSCC and other tumors (30). Our study also shows B2R overexpression in HNSCC. B2R is known to be involved in autocrine or paracrine mechanisms that assist tumor growth, vascular permeability, and metastasis (37), which might relate to cancer survival. However, our data show no association between B2R expression and survival or tumor stage in 43 HNSCC patients. Larger sample sizes with a higher power to determine the relationship between HNSCC patient survival, tumor stage, and B2R overexpression may be necessary to show an association. Alternatively, the level of EGFR expression, which is a major mediator of bradykinin effects, may be a more important factor in patient survival.

Previous studies done in HNSCC, targeting molecules in the above pathway in combination, have shown synergistic antitumor effects. In particular, inhibition of EGFR and COX-2 (19) and inhibition of bradykinin receptor and EGFR (8) have shown increased efficacy in HNSCC. Our study supports the potential for targeting B2R antagonists in combination with EGFR, MEK, or COX-2 inhibitors. Such combination therapies might reduce the dose required for each drug, thus reducing toxicity and enhancing efficacy.

Bradykinin receptor antagonists are already in clinical trials for a number of disorders. The B2R antagonist HOE140 is under clinical trial for the treatment of angioedema (Clinicaltrials.gov Identifier: NCT00097695; currently in phase III studies by Jerini Pharma) and osteoarthritis (Clinicaltrials.gov identifier: NCT00303056) and has also effected improvement in pulmonary function in a clinical trial for asthma (38). Our finding that B2R mediates tumorigenic pathways in HNSCC provides a rationale for additional preclinical studies with B2R antagonists in HNSCC, which could lead to clinical testing for cancer therapy. It is not known if a therapeutic approach using B2R antagonists would be superior to COX-2 inhibition, would be additive with COX-2 or EGFR inhibition, or would have

fewer toxicities than COX-2 inhibitors. Because so many GPCRs can activate EGFR via Src family kinases (8), a Src family kinase inhibitor such as dasatinib may be more beneficial than blocking only one GPCR type, such as B2R, unless a tumor showed particular dependence on the B2R pathway.

Materials and Methods

Materials

Cell culture reagents DMEM, Basal Medium Eagle (BME), and fetal bovine serum were obtained from Invitrogen. B1 and B2 receptor antibodies and their blocking peptides were purchased from Santa Cruz Biotechnology. PY1068-EGFR, Phospho-p42/p44-MAPK and p42/p44-MAPK antibodies and MEK inhibitors, PD98059 and U126, were from Cell Signaling Technology. EGFR antibody and anti-phosphotyrosine antibody (PY20) were purchased from BD Biosciences. COX-2 antibody was from Cayman Chemical Company and β-actin antibody was from Chemicon and Abcam. Antibodies to total and phospho-MAPK were from Cell Signaling. Gefitinib was a gift from Astrazeneca, and the EGFR antibody C225 (Erbitux) was a gift from Imclone. B1R antagonist Lys (Des-Arg^9-Leu^8)-bradykinin and B2R antagonist HOE140 were purchased from Sigma and from Biomol Research Laboratories, respectively. Gefitinib, erlotinib, PD98059 and U126 were dissolved in DMSO and stored in aliquots at −20°C. The bradykinin antagonist CU201 was a kind gift from Dr. Daniel Chan (Department of Medicine, University of Colorado, Denver, CO), the peptides EGF, bradykinin and the B1R agonist Lys (Lys-Des-Arg^9)-bradykinin were purchased from Invitrogen, Bachem, and from Sigma respectively, dissolved in water and stored in aliquots at −80°C. PGE_2 enzyme immunoassay kit was purchased from Cayman Chemical.

Cell Culture

PCI-37A (39), 1483 (40), and UM-22B (41) HNSCC cells were cultured in BME with 1% fetal bovine serum and L-glutamine and serum deprived using BME for 2 to 3 d, followed by stimulation with bradykinin for experiments. HET-1A (42) is an immortalized human esophageal epithelial cell line. For determination of B2R levels, HET-1A, PCI-37A, 1483, and UM-22B cells were grown in DMEM + 10% fetal bovine serum.

Immunohistochemistry

Paraffin-embedded slides with head and neck tumor tissue and adjacent normal control tissue from 43 HNSCC patients were stained with B1R and B2R antibodies. Kidney slides were used as positive controls for B1R and B2R staining. Blocking peptides were used to confirm the specificity of the antibodies for this application. A standard streptavadin-biotin approach was used to stain the slides after microwave pretreatment for antigen retrieval. The slides were examined microscopically and were scored in a blinded fashion using a semiquantitative scoring system. The amount of tumor was scored as a percentage of the overall tumor in the section with positive staining. The intensity of the stain was scored on a scale of 0 to 3, with 0 indicating absent staining and 3 being the highest intensity of staining. An overall staining score was obtained by multiplying the intensity of staining by the percentage of tissue showing that level of intensity. These values for tumor and normal tissue were then compared using the Wilcoxon signed rank test by GraphPad Instat statistical analysis program. $P < 0.05$ was considered statistically significant.

Immunoblotting

Immunoblotting was used to determine the protein levels of EGFR, phosphorylated EGFR, phosphorylated MAPK, and COX-2. Subsequent to treatment with inhibitors and agonists, HNSCC cells were lysed in ice-cold radioimmunoprecipitation assay buffer containing protease inhibitor cocktail tablet (Roche) and phosphatase inhibitors (Na3VO4 and NaF). Proteins were resolved by SDS-PAGE using 6% Tris-glycine gels for EGFR and 10% gels for COX-2, transferred onto nitrocellulose membranes, and blocked with 5% bovine serum albumin (to measure phosphorylated proteins) or 5% milk (to measure total protein levels). Primary antibody diluted in blocking solution was added and incubated overnight. Horseradish peroxidase–conjugated secondary antibody was then used, followed by chemiluminescent detection using the ECL kit (Amersham). In some experiments, total phosphorylation of EGFR was determined by immunoprecipitation and immunoblotting with an antibody to phospho-tyrosine. EGFR protein was first immunoprecipitated with 1.2 μg of anti-EGFR antibody and resolved on an 8% SDS-PAGE gel. Following transfer to nitrocellulose membrane, the membrane was blocked in 5% Blotto solution and probed with 1:1,000 dilution of anti-phosphotyrosine (PY20) antibody.

Protein levels of B2R were compared between tumor and normal tissues for each head and neck cancer patient by immunoblotting. For this experiment, tumor and normal tissues were obtained from six head and neck cancer patients. The tissue lysates were resolved by SDS-PAGE and probed with B1R and B2R antibodies (dilution of 1:200) and β-actin antibody (dilution of 1:10,000). Densitometric analysis of the blots was done using the ScionImage program, which yielded numerical values that were plotted to generate graphs. The same immunoblotting method was followed to determine the levels of these receptors in lysates of head and neck cell lines HET-1A, 1483, PCI-37A, and UM-22B.

Specificity of the B2R antibody was confirmed by peptide competition. For this experiment, B2R antibody was preincubated with a five-fold excess of B2R blocking peptide. This mixture was added to a blot containing cell lysate proteins and incubated overnight; another identical blot was incubated in parallel with B2R antibody alone. Absence of the 75-kDa B2R band in the blot incubated with blocking peptide plus antibody was used to show the specificity of the antibody for B2R.

ELISA

For the detection of PGE_2 release, PCI-37A cells were grown in 60 × 60-mm dishes to 75% confluence and then serum deprived for 48 h. The culture medium was replaced with 3 mL of serum-free fresh BME, and bradykinin (10 nmol/L) was added. After treatment for the indicated time period, the supernatants were harvested and stored at −80°C until subsequent assay of PGE_2 release. The same cells were also

cultured in a similar manner to examine COX-2 protein expression by immunoblot. Fifty microliters of supernatant from each sample were used for analysis of PGE_2 using a PGE_2 EIA kit (Cayman Chemicals) following the manufacturer's instruction. Briefly, 50 μL of the medium, along with a serial dilution of PGE_2 standard samples, were mixed with appropriate amounts of the AchE Tracer and PGE_2 antiserum and incubated at 4°C on a shaker for 18 h. After the wells were emptied and rinsed with wash buffer, 200 μL of Ellman's reagent containing substrate for acetylcholinesterase were added. The enzyme reaction was carried out on a slow shaker at room temperature for 1.5 h. The absorbance at 405 nm was determined using a Wallac Victor^2 1420 Multilabel Counter (Perkin-Elmer). Assays were done in duplicate and are expressed as picograms per milliliter.

Statistical Analysis

Values shown represent the means ± SDs. Statistical analysis for biochemical assays was done by Student's t test, with $P < 0.05$ being considered statistically significant. Statistical determinations for immunohistochemical staining results were carried out by Wilcoxon signed rank test using GraphPad Instat statistical analysis program to evaluate the staining score between tumor and normal tissues. $P < 0.05$ was considered statistically significant.

Disclosure of Potential Conflicts of Interest

No potential conflicts of interest were disclosed.

References

1. Darmoul D, Gratio V, Devaud H, Laburthe M. Protease-activated receptor 2 in colon cancer: trypsin-induced MAPK phosphorylation and cell proliferation are mediated by epidermal growth factor receptor transactivation. J Biol Chem 2004; 279:20927–34.

2. Fischer OM, Hart S, Gschwind A, Ullrich A. EGFR signal transactivation in cancer cells. Biochem Soc Trans 2003;31:1203–8.

3. Gschwind A, Prenzel N, Ullrich A. Lysophosphatidic acid-induced squamous cell carcinoma cell proliferation and motility involves epidermal growth factor receptor signal transactivation. Cancer Res 2002;62:6329–36.

4. Raj GV, Barki-Harrington L, Kue PF, Daaka Y. Guanosine phosphate binding protein coupled receptors in prostate cancer: a review. J Urol 2002; 167:1458–63.

5. Venkatakrishnan G, Salgia R, Groopman JE. Chemokine receptors CXCR-1/2 activate mitogen-activated protein kinase via the epidermal growth factor receptor in ovarian cancer cells. J Biol Chem 2000;275:6868–75.

6. Li S, Huang S, Peng SB. Overexpression of G protein-coupled receptors in cancer cells: involvement in tumor progression. Int J Oncol 2005;27: 1329–39.

7. Krysan K, Reckamp KL, Dalwadi H, et al. Prostaglandin E_2 activates mitogen-activated protein kinase/Erk pathway signaling and cell proliferation in non-small cell lung cancer cells in an epidermal growth factor receptor-independent manner. Cancer Res 2005;65:6275–81.

8. Thomas SM, Bhola NE, Zhang Q, et al. Cross-talk between G protein-coupled receptor and epidermal growth factor receptor signaling pathways contributes to growth and invasion of head and neck squamous cell carcinoma. Cancer Res 2006;66:11831–9.

9. Taub JS, Guo R, Leeb-Lundberg LM, Madden JF, Daaka Y. Bradykinin receptor subtype 1 expression and function in prostate cancer. Cancer Res 2003; 63:2037–41.

10. Zhao Y, Xue Y, Liu Y, et al. Study of correlation between expression of bradykinin B2 receptor and pathological grade in human gliomas. Br J Neurosurg 2005;19:322–6.

11. Wu J, Akaike T, Hayashida K, et al. Identification of bradykinin receptors in clinical cancer specimens and murine tumor tissues. Int J Cancer 2002;98: 29–35.

12. Exton JH. Phospholipase D-structure, regulation and function. Rev Physiol Biochem Pharmacol 2002;144:1–94.

13. Barki-Harrington L, Bookout AL, Wang G, Lamb ME, Leeb-Lundberg LM, Daaka Y. Requirement for direct cross-talk between B1 and B2 kinin receptors for the proliferation of androgen-insensitive prostate cancer PC3 cells. Biochem J 2003;371:581–7.

14. Greco S, Muscella A, Elia MG, Romano S, Storelli C, Marsigliante S. Mitogenic signalling by B2 bradykinin receptor in epithelial breast cells. J Cell Physiol 2004;201:84–96.

15. Chen BC, Yu CC, Lei HC, et al. Bradykinin B2 receptor mediates NF-κB activation and cyclooxygenase-2 expression via the Ras/Raf-1/ERK pathway in human airway epithelial cells. J Immunol 2004;173:5219–28.

16. Chan G, Boyle JO, Yang EK, et al. Cyclooxygenase-2 expression is up-regulated in squamous cell carcinoma of the head and neck. Cancer Res 1999;59: 991–4.

17. Zhang X, Chen ZG, Choe MS, et al. Tumor growth inhibition by simultaneously blocking epidermal growth factor receptor and cyclooxygenase-2 in a xenograft model. Clin Cancer Res 2005;11:6261–9.

18. Vane JR, Bakhle YS, Botting RM. Cyclooxygenases 1 and 2. Annu Rev Pharmacol Toxicol 1998;38:97–120.

19. Choe MS, Zhang X, Shin HJ, Shin DM, Chen ZG. Interaction between epidermal growth factor receptor- and cyclooxygenase 2-mediated pathways and its implications for the chemoprevention of head and neck cancer. Mol Cancer Ther 2005;4:1448–55.

20. Yu H, Carretero OA, Juncos LA, Garvin JL. Biphasic effect of bradykinin on rabbit afferent arterioles. Hypertension 1998;32:287–92.

21. Bawolak MT, Gera L, Morissette G, Stewart JM, Marceau F. B-9972 is an inactivation-resistant agonist of the bradykinin B2 receptor derived from the peptide antagonist B-9430. J Pharmacol Exp Ther 2007;323: 534–46.

22. Siegfried JM, Gubish CT, Rothstein ME, Queiroz de Oliveira PE, Stabile LP. Signaling pathways involved in cyclooxygenase-2 induction by hepatocyte growth factor. Mol Pharmacol 2007;72:769–79.

23. Simpson PB, Woollacott AJ, Hill RG, Seabrook GR. Functional characterization of bradykinin analogues on recombinant human bradykinin B(1) and B(2) receptors. Eur J Pharmacol 2000;392:1–9.

24. Hock FJ, Wirth K, Albus U, et al. Hoe 140 a new potent and long acting bradykinin-antagonist: *in vitro* studies. Br J Pharmacol 1991;102: 769–73.

25. Zhang SP, Codd EE. Characterization of bradykinin receptors in human lung fibroblasts using the binding of 3[H] [Des-Arg10, Leu9]kallidin and 3[H]NPC17731. Life Sci 1998;62:2302–14.

26. Leeb-Lundberg LM, Marceau F, Muller-Esterl W, Pettibone DJ, Zuraw BL. International union of pharmacology. XLV. Classification of the kinin receptor family: from molecular mechanisms to pathophysiological consequences. Pharmacol Rev 2005;57:27–77.

27. Rubin Grandis J, Melhem MF, Gooding WE, et al. Levels of TGF-α and EGFR protein in head and neck squamous cell carcinoma and patient survival. J Natl Cancer Inst 1998;90:824–32.

28. Ikeda Y, Hayashi I, Kamoshita E, et al. Host stromal bradykinin B2 receptor signaling facilitates tumor-associated angiogenesis and tumor growth. Cancer Res 2004;64:5178–85.

29. Dlamini Z, Bhoola K. Esophageal cancer in African blacks of Kwazulu Natal, South Africa: an epidemiological brief. Ethn Dis 2005;15:786–9.

30. Dannenberg AJ, Lippman SM, Mann JR, Subbaramaiah K, DuBois RN. Cyclooxygenase-2 and epidermal growth factor receptor: pharmacologic targets for chemoprevention. J Clin Oncol 2005;23:254–66.

31. Wang D, Buchanan FG, Wang H, Dey SK, DuBois RN. Prostaglandin E_2 enhances intestinal adenoma growth via activation of the Ras-mitogen-activated protein kinase cascade. Cancer Res 2005;65:1822–9.

32. Batzer AG, Rotin D, Urena JM, Skolnik EY, Schlessinger J. Hierarchy of binding sites for Grb2 and Shc on the epidermal growth factor receptor. Mol Cell Biol 1994;14:5192–201.

33. Kloth MT, Laughlin KK, Biscardi JS, Boerner JL, Parsons SJ, Silva CM. STAT5b, a mediator of synergism between c-Src and the epidermal growth factor receptor. J Biol Chem 2003;278:1671–9.

34. Boerner JL, Biscardi JS, Silva CM, Parsons SJ. Transactivating agonists of the EGF receptor require Tyr 845 phosphorylation for induction of DNA synthesis. Mol Carcinog 2005;44:262–73.

35. Han JW, Sadowski H, Young DA, Macara IG. Persistent induction of cyclooxygenase in p60v-src-transformed 3T3 fibroblasts. Proc Natl Acad Sci U S A 1990;87:3373–7.

36. Moraitis D, Du B, De Lorenzo MS, et al. Levels of cyclooxygenase-2 are increased in the oral mucosa of smokers: evidence for the role of epidermal growth factor receptor and its ligands. Cancer Res 2005;65:664–70.

37. Naidoo S, Raidoo DM. Tissue kallikrein and kinin receptor expression in an angiogenic co-culture neuroblastoma model. Metab Brain Dis 2006;21:253–65.

38. Akbary AM, Wirth KJ, Scholkens BA. Efficacy and tolerability of Icatibant (Hoe 140) in patients with moderately severe chronic bronchial asthma. Immunopharmacology 1996;33:238–42.

39. Heo DS, Snyderman C, Gollin SM, et al. Biology, cytogenetics, and sensitivity to immunological effector cells of new head and neck squamous cell carcinoma lines. Cancer Res 1989;49:5167–75.

40. Sacks PG, Parnes SM, Gallick GE, et al. Establishment and characterization of two new squamous cell carcinoma cell lines derived from tumors of the head and neck. Cancer Res 1988;48:2858–66.

41. Grenman R, Carey TE, McClatchey KD, et al. *In vitro* radiation resistance among cell lines established from patients with squamous cell carcinoma of the head and neck. Cancer 1991;67:2741–7.

42. Stoner GD, Kaighn ME, Reddel RR, et al. Establishment and characterization of SV40 T-antigen immortalized human esophageal epithelial cells. Cancer Res 1991;51:365–71.

Molecular Cancer Research

Kinin B2 Receptor Mediates Induction of Cyclooxygenase-2 and Is Overexpressed in Head and Neck Squamous Cell Carcinomas

Weiping Zhang, Neil Bhola, Shailaja Kalyankrishna, et al.

Mol Cancer Res 2008;6:1946-1956.